2023 IEEE/ASME International Conference on Advanced Intelligent Mechatronics (AIM)
June 28-30, 2023. Seattle, Washington, USA

Development of a Long Flexible Manipulator Utilizing the Motions of Twining and Tightening to Enhance Holding Ability

Shotaro SHIMEGI
Department of Modern Mechanical Engineering
Waseda University
TOKYO, JAPAN
ssbb13202@sagi.waseda.jp

Keitaro ISHIBASHI
Department of Modern Mechanical Engineering
Waseda University
TOKYO, JAPAN
ishibashi-k@asagi.waseda.jp

Toshihiro USAMI
Department of Modern Mechanical Engineering
Waseda University
TOKYO, JAPAN
usa-toshihiro@ruri.waseda.jp

Hiroyuki ISHII
Department of Modern Mechanical Engineering
Waseda University, and the Human Robotics Institute (HRI)
TOKYO, Japan
hiro.ishii@waseda.jp

***Abstract*— Many researchers have been studying long and flexible robots, such as snake-like robots and continuum manipulators. The feature of continuum robots is flexibility; therefore, high rigidity has been considered a characteristic to be avoided or unavoidably accepted for controllability. We envisioned a continuum manipulator that takes advantage of both high rigidity and flexibility to enhance its abilities. This paper proposes a concept and an integration method of a new long and flexible manipulator, named Robotic Whip, utilizing both flexible motion and tightening by increasing rigidity. The prototype is 1.4 m in length and 647 g in weight and is actuated by three DC motors rotating winches. Pulling wires enable the device to exhibit an active tightening motion, and loosening wires enable a flexible twining motion. In addition, we estimated the flexible motion of the continuum arm, which consisted of 200 originally designed links, using a simulation based on a rigid links model. Through experiments, it was proven that the prototype performance was adequate, and the device twined around the target bar and enhanced its holding ability by tightening the bar to tow a dolly with a mass of above 2 kg. A comparison of the simulation and actual measurement results showed that our model could reduce the number of prototypes by clarifying the device specifications available for a given situation.**

I. INTRODUCTION

Over the years, human beings have made and used tools, such as stone tools, earthenware, and ropes. To improve our lives, we polish our various skills, build up our techniques, and create even more useful and more usable tools. As time passed, metals and plastic became the main materials of parts, and electrical energy has made tools smaller and more powerful; thus, tools have become more complex and sophisticated entities called "devices." While new machines are generated along with developing processing techniques and new technologies, such as robotics, we can still see scenes today that show the effectiveness of the oldest tools. Long flexible tools, such as ropes and strings, are prime examples. These tools have continuum bodies that are considered as many small rigid bodies in a model. Because of their many degrees of freedom, continuum bodies are difficult to actuate precisely, and their shape cannot be easily prevented from being deformed by external forces. However, there are various advantages to the properties afforded by these redundancies, and many researchers have studied robots with long, flexible movements. Snake-like robots are an attractive research topic for researchers, who have suggested theories and prototyping for a long time [1]–[6]. The ACM series [7], [8] is a typical example of a robot that accurately reproduces the movements of a snake. In addition, Takemori [9] proposed a method of moving over obstacles that utilizes snake tightening, in which the robot enhances its own friction force to prevent falling. Some researchers have studied softer and more flexible robots called continuum robots [10]–[14]. Greer [15] developed a rubber robot that can extend from the tip and move while avoiding obstacles. Onda [16] used a continuum mechanism for a narrow robot with non-contact propulsion. Owing to their flexibility, these robots have been developed to be more flexible, and high rigidity has been considered a characteristic to be avoided or traded off for controllability.

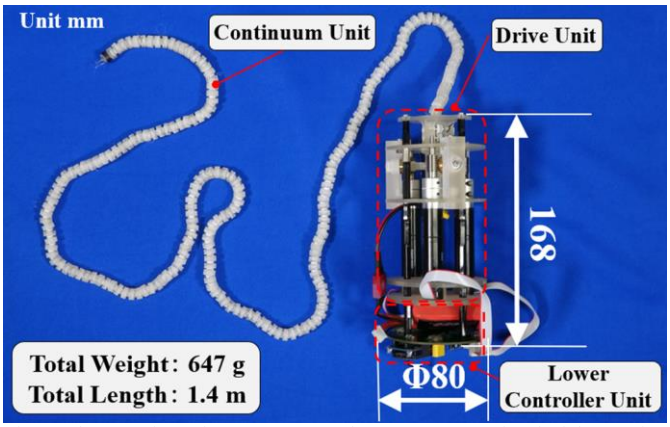

Fig. 1. The overview of our prototype. The prototype consisted of three unit: Drive Unit, Continuum Unit, and Lower Controller Unit.

In this paper, we propose a new long flexible device called robotic whip. Robotic Whip consists of several rigid links connected by three wires that are driven by DC motors. This device can move flexibly and passively first by being swept

This work was supported in part by the JSPS KAKENHI under Grants 19H01130, and 21H05055, and in part by the Waseda University Grant for Special Research Projects under Project 2021C-177.

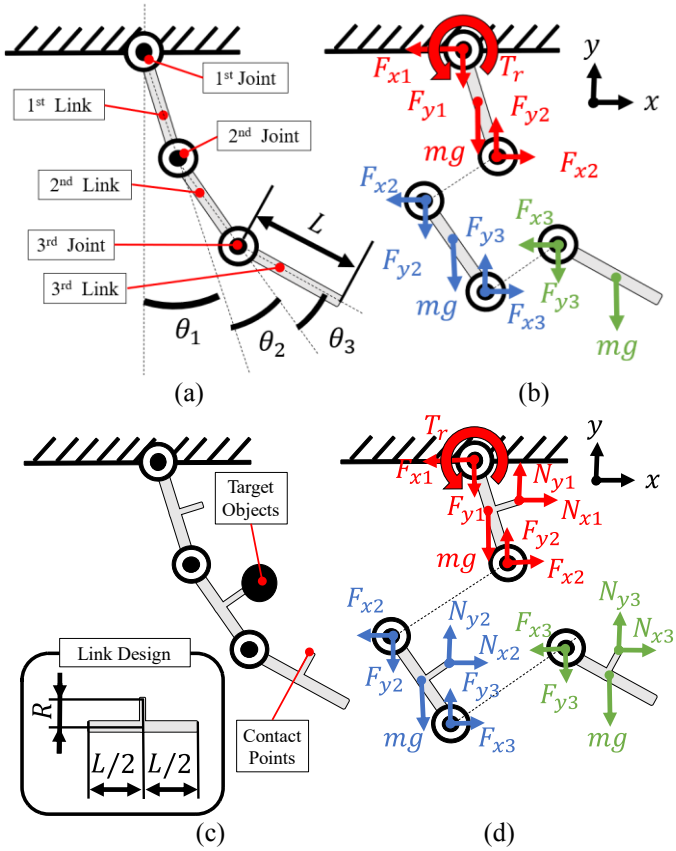

Fig. 2. Modeling for each motion. (a) Name of parts. Each part is regarded as a set of one rigid link and one rotary joint. (b) Free body diagram. (c) (d) Contact forces to the target object.

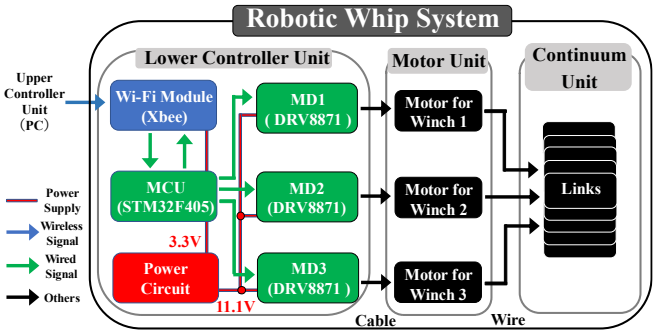

Fig. 3. Complete system of robotic whip. This robotic tool follows the order from users through an upper controller unit.

away and twining around an elongated object like a bar. Then, the integrated motors and winches pull the wire and strengthen the overall stiffness so that the robotic whip can tighten elongated objects like a snake and enhance its grasping ability. The contribution of this study is an integration method that enables both the flexibility of a real rope and rigidity to tow a cart. A mobile application with a continuum mechanism has similar conflicting expectations in holding ability. Many soft, long manipulators can enhance their grasping ability, similar to our prototype. In Section II, we explain our conceptual model for each motion: flexible passive motion and tightening active motion. Section III presents the entire system of our prototype and a hardware design for switching stiffness consisting of three units: Continuum Unit (CU), Lower Controller Unit (LCU), and Motor Unit (MU). Sections IV and V discuss the results of the experiments and performance of the integrated devices. Section VI provides a summary of this paper.

II. Modeling

The model of a continuum manipulator varies depending on the research purpose and mechanical design [11], [17], [18]. Because our prototype contacts the bar and must have sufficient stiffness to tighten the object and hold it, we use a basic rigid link model to estimate the motion of the continuum manipulator. To simplify the calculations, the friction and resistance components, which were considered to have little effect, were omitted from the display, and the focus was on estimating an overview of the motion. This model is basic but can accommodate an increasing number of links. Through this model and simulation, we can focus on fewer trial and error and more purposeful integration.

A. Flexible Motion

The objective of this model is to estimate the coiling motion when the inputs are the length and number of links, size of the object, and distance to the object. Fig. 2 shows our basic rigid-link model for a continuum manipulator, which is regarded as an assembly of links and rotary joints. Each link has a force interaction through each joint, gravity force, and external force generated by the contacting objects. The equations for the first link are as follows:

$$m_1\ddot{x}_1 = -F_{x1} + N_{x1} + F_{x2} \quad (1)$$

$$m_1\ddot{y}_1 = m_1 g + F_{y1} - N_{y1} + F_{y(i+1)} \quad (2)$$

$$I_1\ddot{\theta}_1 = T_r + \left\{(F_{x1} + F_{x2})\frac{L}{2} + N_{y1}R\right\}cos\theta_1 + \left\{(F_{y1} + F_{y2})\frac{L}{2} - N_{x1}R\right\}sin\theta_1 \quad (3)$$

The equations for middle link i ($i = 2, 3\ldots$) are as follows:

$$m_i\ddot{x}_i = -F_{xi} + N_{xi} + F_{x(i+1)} \quad (4)$$

$$m_i\ddot{y}_i = m_i g + F_{yi} - N_{yi} + F_{y(i+1)} \quad (5)$$

$$I_i\ddot{\theta}_i = \left\{(F_{xi} + F_{x(i+1)})\frac{L}{2} + N_{yi}R\right\}cos\sum\theta_i + \left\{(F_{yi} + F_{y(i+1)})\frac{L}{2} - N_{xi}R\right\}sin\sum\theta_i \quad (6)$$

where m_i[kg] is the mass of link i, g[m/s^2] is the gravitational acceleration, I_i[kg · m^2] is the inertia of link i, F_{xi} and F_{yi} [N] are the joint reaction forces, T_r is the swinging torque by users, N_{xi} and N_{yi} [N] are the external forces due to the contact and wire tension, respectively, and R and L [m] are the lengths from the link design.

In flexible motion, the continuum arm moves passively according to the torque of the first joint and can twine round objects if some of the pre-contact conditions are met, such as the initial speed, the link's number of first contacts, and the ratio of the length of links to the perimeter of the object.

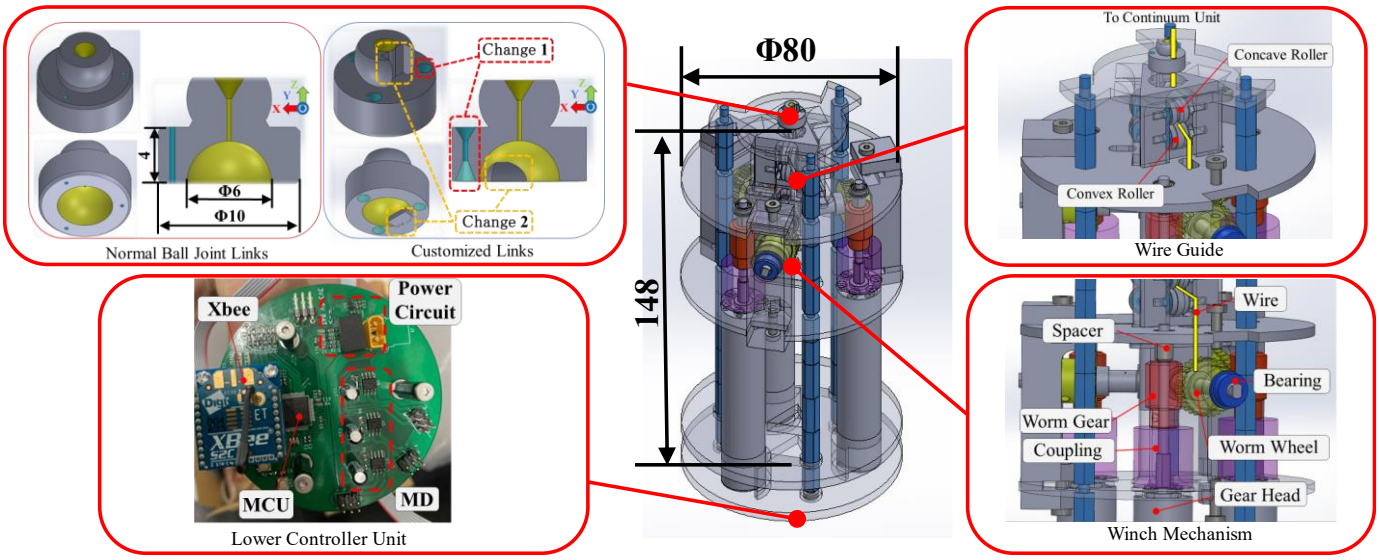

Fig. 4. The summary of the hardware design. 200 links are used in CU. MU has two important roles. LCU is designed originally for this prototype.

B. *Tightening Motion*

Tightening is a complex motion that includes both passive and active motion. The first action is to generate external forces to bend the continuum arm using a wire. The wire creates not only forces but also geometric constraints; thus, a continuum manipulator that has already twinned around the target can tighten the target object while conforming to the shape of the target. The forces exerted by the wire are represented in the model as externally acting forces. As with the forces acting by contact, only one point of action is considered for each link.

III. Mechanical Design and System Integration

The prototype of the robotic whip has a 1.4 m length and a mass of 647 g, including the battery mass (Fig.1). This device consists of three units: Continuum Unit (CU), Motor Unit (MU), and Lower Controller Unit. (Fig.3). CU is a soft manipulator that can hold and tighten an object. MU has three motors and a winch mechanism that generates wire forces by winding the wires. LCU is a circuit that receives messages from users via wireless communication and controls motors using rotary sensors.

A. *Continuum Unit*

CU consists of 200 rigid links, the design of which is inspired by Variable Stiffness Mechanism [12]. The normal ball joint link (NBJL) was expanded to allow the core rod and three pull wires to pass through. Another customized link (CL) was further improved to reduce the friction of the pull wires and the torsion of the CU. Both were made of Acrylic-based UV-curable resin using a 3D printer. The length of this unit, which has 200 joints, is approximately 1.2 m; therefore, the friction loss in each joint affects the total flexibility and efficiency of movement.

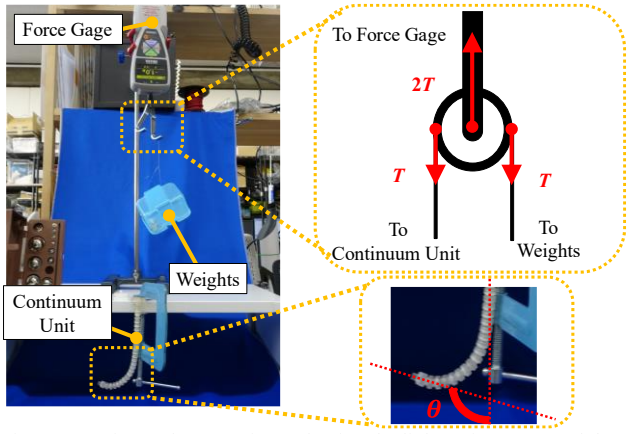

Fig. 5. Experimental system for evaluating the link performance and the principal model measuring the forces using a fixed pulley.

B. *Motor Unit*

MU actuates CU by winching wires and transmitting pulling forces to the links. A gearhead attached to the DC motor generates the first actuation from electrical energy and transmits a rotational force to the worm gear through coupling. Then, the worm wheel starts to rotate and winch the wire. The winched wire passed the wire guide, which consisted of a pair of uneven convex rollers. Guided wires were arranged concentrically and connected to CU. Frame parts are made by, similar to links, Acrylic-based UV-curable resin using a 3D printer, and mechanical components such as gears, shafts, and coupling are made by Sus to ensure sufficient rigidity.

C. *Lower Controller Unit*

LCU was attached to the bottom of MU and played an important role in the operation of this device. First, the unit receives orders from users via Upper Controller Unit (UCU). Second, the MCU judges the next control action, which is the motor actuation. The MCU then controls the motor based on the data from a rotary sensor on the motor. The electric energy

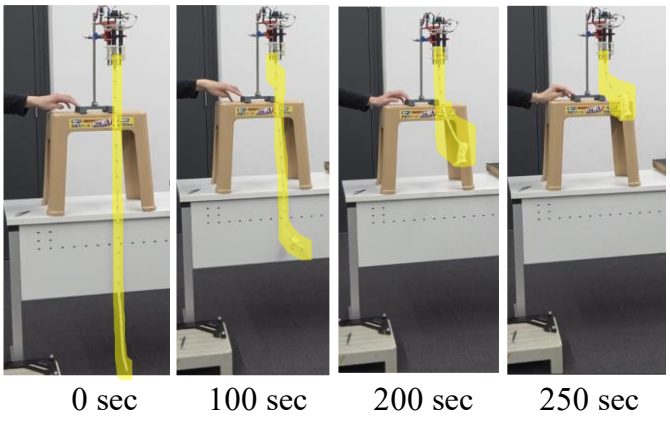

Fig. 6. Experimental system for evaluating the motor unit performance and the coiling motion of continuum unit by motor actuation.

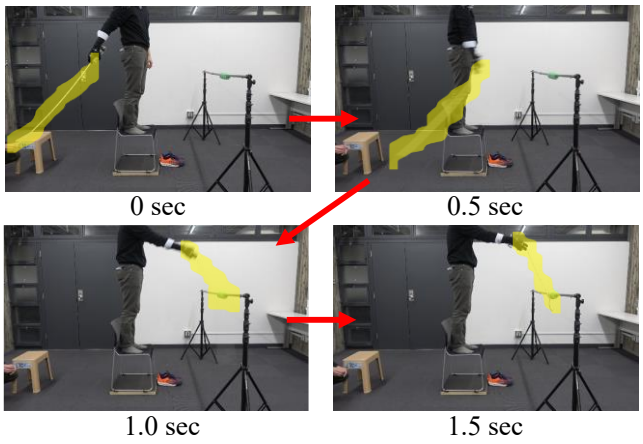

Fig. 7. Experiment for flexible twining motion by user's throwing. Motion is measured by motion capture system with cameras and seals.

source is a Li-Po battery, which has three cells (11.1V), 35C, and 450mAh, and is shared between the motors and controllers; thus, LCU has a two-stage buck circuit composed of a DCDC converter and a linear regulator. The high conversion efficiency electrical circuit connects the lightweight battery with the high portability of the device.

IV. Experiment

A. Link Perfomance

There is a complex relationship between the wire pulling forces and the bending angle of CU because the link has a friction force dependent on the method of contact with the wires. Therefore, we conducted an experiment to evaluate our design improvement and compare the characteristics of an assembly of 27 NBJL to those of a 27 CL, in which the continuum can bend at 810°. Fig. 5 shows the experimental system used to measure the link performance. The initial state of the CU adjusted manually was a straight line in the gravity direction or a slight bend in the bending direction. The pulling force was added to the weights and measured accurately using a force gauge. Bending angles were measured from the images. We then increased the weights repeatedly until the total mass was 570 g, including the weight case.

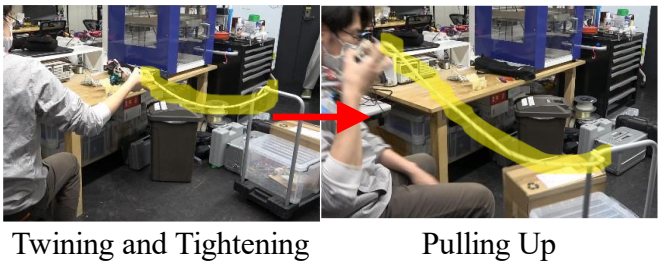

Fig. 8. Total demonstration of the prototype after integrating all system. Holding ability was enhanced by tightening after twining around the dolly handle and enable user to pull the dolly.

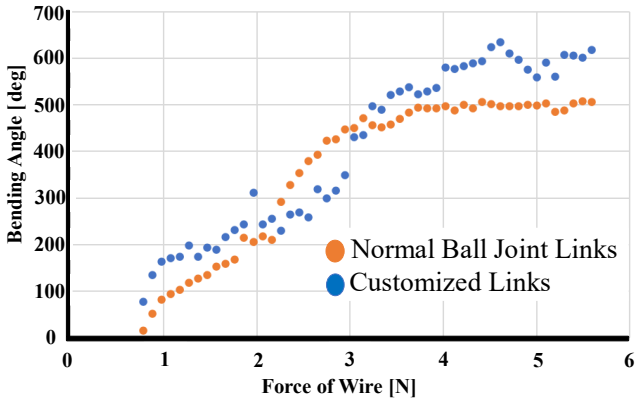

Fig. 9. The measured relationship between pulling force and bending angle. Orange plots show the results of NBJL. Blue plots show those of CL.

B. MU Perfomance

A common problem in small devices is the relationship between battery size and output power. For high portability, a smaller battery is a better method; however, a larger battery is required for high performance. Therefore, we checked our prototype's ability using the selected battery after complete integration. Fig. 6 shows the experimental system and movement of the prototype actuated by the motor. First, we set the prototype to stage and manually adjusted the direction of CU it was straight. Second, one motor started to winch and pull wires. Then, the CU started to bend, and we observed the maximum degree and factor in the performance limit.

C. Flexible Twining around The Bar

To verify the results of our model and simulation, a flexible motion experiment was conducted using a 3D motion capture system called OptiTrack (Fig.7). In this experiment, the target object was a bar with a diameter of 60 mm that was positioned at a distance and height of 800 mm from the user's shoulder. The user stood on the char to exclude the effects of contact between the prototype and the ground. The assistant made the initial state of the prototype in-line with the arms of the attached user. As soon as the assistant released his hand, the user turned only in one direction, while maintaining the elbow and wrist posture, and coiled the prototype around the stick. The motion of the shoulders and 20 links positioned equally in this sequence of actions was measured using the motion capture system.

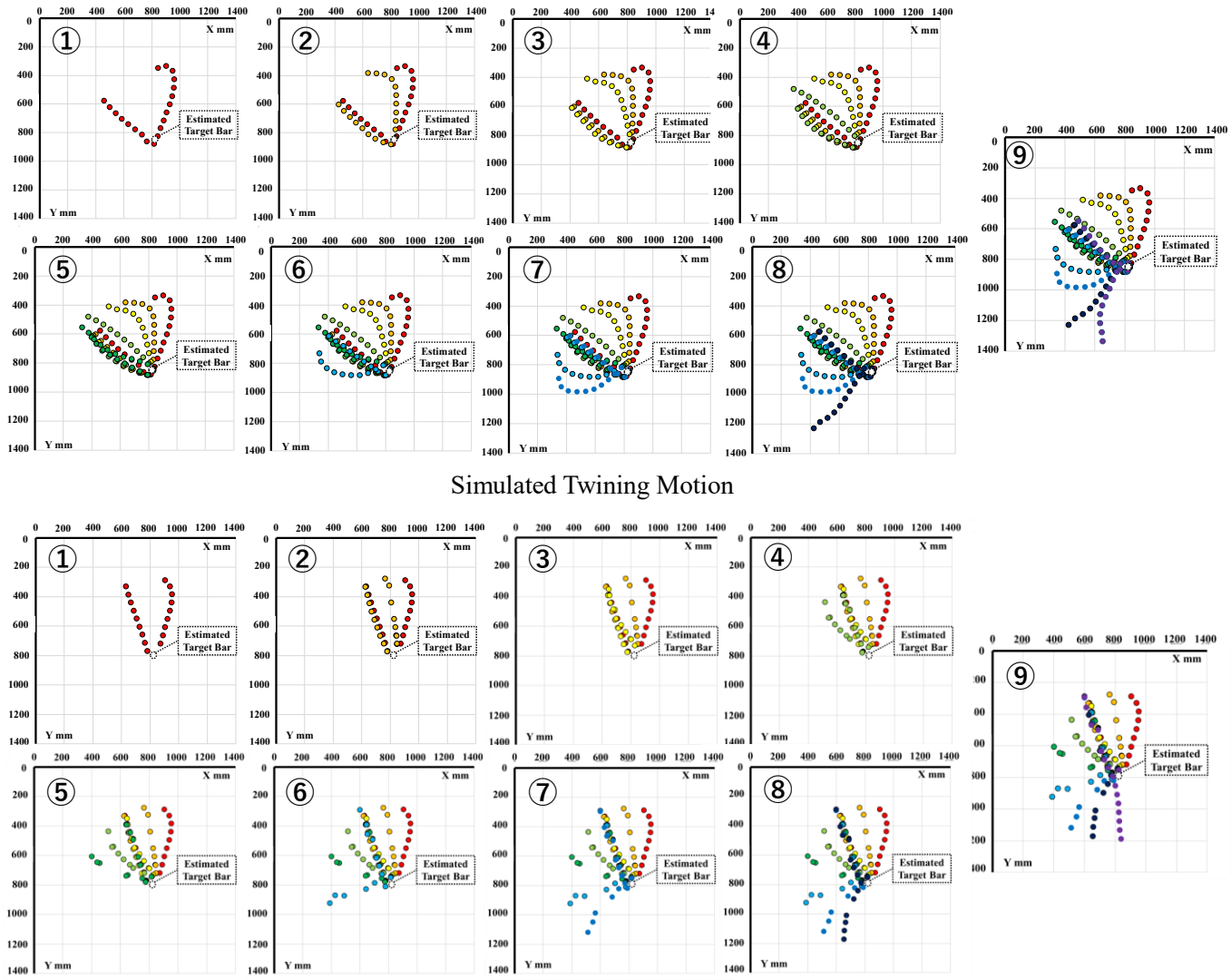

Fig. 10. The simulation and experimental plots for the flexible twining around the bar in the time sequence. The simulation results were calculated using MATLAB and plotted using Excel. The plotting occurs 0.2 sec the twinning around the bar began.

D. Integration Demonstration

To demonstrate the enhanced holding ability resulting from integration, a demonstration with traction was conducted (Fig. 8). The experimental procedure was almost the same as in the previous section, but the difference was that the user's state in the former demonstration closely approximated daily life, and the bar was also a dolly handle with a mass of above 2 kg.

V. Discussion

A. The effects of link design improvement

CL was improved to reduce the effects of the friction force. Fig. 9 shows the relationship between the force and tip angles of NBJL and CL. There were two distinctive features in the plots. One is the total offset that the blue plots have, especially in the stable lower and upper ranges. This feature indicates that the CU consisting of the CL requires less force to obtain the desired angle. The second feature is the slope of the change state outside the previous range. As the bending angle increases and the pulling force increases, the value of the slope becomes positive. The slope in blue is larger than that in orange. This means that CL is straightforward and reacts sensitively to external forces and gravity.

B. 3-Dimensional twist and Performance Improvement

As shown in Fig. 6, CU can coil 10 times (3600 °) by motor actuation until the wires snap at a force of 37 N. However, this unit also twists like a snake, despite the existence of a twisting guard. This phenomenon is due to the design margin and is created by the redundancies inherent in continuum manipulators; however, it is an essential element of the characteristic tightening of the device. There is a ±0.05 mm margin for the unevenness of the twisting guard; therefore, a pair of CLs can twist ±1.15 °. Because the CU consists of 200 links, the total allowance twist degree is ±230 °, which enables

CU to avoid contacting itself in the twinning around a bar. To enhance the holding ability and stabilize the twining state, there should be more coils on the target. In fact, demonstrations have been able to tow a dolly by twining around it about 2 times. Further research into the models and conditions involved will enhance the usefulness of this device, particularly by adding the operating time and circuit model, in addition to improving the performance of mobile devices.

C. Comparison of simulated and measured twining motions

Fig. 10 shows two plots that represent the simulation and experimental results of when CU twined around the bar. The simulation results based on a rigid-link model, described in Section II and shown in Fig. 2, was calculated using MATLAB and plotted in Excel, similar to the measurement. From the overview of the comparison, we can state that the general motions are in well agreement after contact and twinning; however, some plots in the measurement results were lost because they entered the blind spot of the experimental instrument. Based on this comparison, it is proven that our simulation method can support the reduction of the number of prototypes when the main inputs and conditions, such as distance to the object and user movement, are known. There was a slight difference in the flexibility of the tip. The cause is presumed to be the bending rigidity derived from the wires and core material or the resistance component owing to the friction of the ball joint. In the future, we will accurately incorporate this resistance component into the model and predict the trajectory of flexible motion that accompanies changes in stiffness derived from the application of wire tension considering 3-dimension twists.

VI. Conclusion

We described a new flexible device, named Robotic Whip, which can change its rigidity by the actuation of wires, and a method to integrate this mobile system. To estimate the flexible motions of the CU, we propose a method that uses a basic rigid-link model, considering an increased number of links and contact with the targets. This device is made mainly from Acrylic-based UV-curable resin to reduce weight, has a length of 1.4 m, mass of 647 g, three actuated DC motors, and a lightweight battery. Through the experiments, it was proven that the prototype of the Robotic Whip can move passively by the user's swing and can enhance its own holding ability by actively tightening to the extent that the dolly with a mass of above 2kg can be pulled. In addition, the passive twining motion can be estimated using MATLAB, which reduces the number of prototypes, as the prototype specifications can be selected according to the specified situation and operation in advance. The main contribution of this study is an integration method for a mobile continuum manipulator with a long length that can enhance the holding ability by twining and tightening.

References

[1] J. GRAY, "The mechanism of locomotion in snakes.," J Exp Biol, vol. 23, no. 2, 1946, pp. 101–120

[2] S. Hirose and M. Mori, "Biologically inspired snake-like robots," pp. 1–7, 2004.

[3] B. Liz, "a 3-Dimensional Snake-like Robot," in International Conference on Robotics & Automation, 2003, pp. 2067–2072.

[4] R. J. Webster, A. M. Okamura, and N. J. Cowan, "Toward Active Cannulas: Miniature Snake-like Surgical Robots," in IEEE International Conference on Intelligent Robots and Systems, 2006, pp. 2857–2863.

[5] R. Worst, R. Linnemann, and D.-S. Augustin, "Construction and Operation of a Snake-like Robot," in IEEE International Joint Symposia on Intelligence and Systems, 1996, pp. 164–169.

[6] S. Ma, Y. Ohmarneuda, K. Inoue, and B. Liz, "Control of a 3-Dimensional Snake-like Robot," in IEEE International Conference on Robotics &Automation, 2003, pp. 2067–2072.

[7] T. Ohashi, H. Yamada, and S. Hirose, "Loop Forming Snake-like Robot ACM-R7 and its Serpenoid Oval Control," IEEE/RSJ 2010 International Conference on Intelligent Robots and Systems, IROS 2010 - Conference Proceedings, 2010, pp. 413–418.

[8] H. Komura, H. Yamada, and S. Hirose, "Development of snake-like robot ACM-R8 with large and mono-tread wheel," Advanced Robotics, vol. 29, no. 17, pp. 1081–1094, Sep.2015.

[9] T. Takemori, M. Tanaka, and F. Matsuno, "Gait Design of a Snake Robot by Connecting Simple Shapes," SSRR 2016 - International Symposium on Safety, Security and Rescue Robotics, 2016, pp. 189–194.

[10] Y. Kim, G. A. Parada, S. Liu, and X. Zhao, "Ferromagnetic soft continuum robots," Sci Robot, vol. 4, no. 33, p. eaax7329, 2019.

[11] K. Hsiao and H. Mochiyama, "A Wire-driven Continuum Manipulator Model without assuming shape curvature constancy," IEEE International Conference on Intelligent Robots and Systems, vol. 2017-Septe, pp. 436–443, 2017.

[12] K. Tadakuma, T. Fujimoto, M. Watanabe, T. Shimizu, E. Takane, M. Konyo, and S. Tadokoro, "Fire-Resistant Deformable Soft Gripper Based on Wire Jamming Mechnism," 2020 3rd IEEE International Conference on Soft Robotics (RoboSoft), vol. 1, 2020.

[13] K. Hatazaki, M. Konyo, K. Isaki, S. Tadokoro, and F. Takemura, "Active Scope Camera for Urban Search and Rescue," IEEE International Conference on Intelligent Robots and Systems, 2007, pp. 2596–2602.

[14] Y. Satake, A. Takanishi, and H. Ishii, "Novel Growing Robot with Inflatable Structure and Heat-Welding Rotation Mechanism," IEEE/ASME Transactions on Mechatronics, vol. 25, no. 4, 2020, pp. 1869–1877.

[15] J. D. Greer, T. K. Morimoto, A. M. Okamura, and E. W. Hawkes, "A soft, steerable continuum robot that grows via tip extension," Soft Robot, vol. 6, no. 1, pp. 95–108, Feb. 2019, doi: 10.1089/soro.2018.0034.

[16] I. Onda, M. Watanabe, K. Tadakuma, E. Takane, M. Konyo, and S. Tadokoro, "Pneumatic Driven Hollow Variable Stiffness Mechanism Aiming Non-contact Insertion of Telescopic Guide Tubes," in 2021 IEEE 4th International Conference on Soft Robotics, RoboSoft 2021, Apr. 2021, pp. 615–621.

[17] N. Lotti et al., "Adaptive Model-Based Myoelectric Control for a Soft Wearable Arm Exosuit: A New Generation of Wearable Robot Control," IEEE Robot Autom Mag, vol. 27, no. 1, Mar. 2020, pp. 43–53.

[18] O. A. Moussa, M. A. Mira, A. H. Fahmy, E. I. Morgan, and O. M. Shehata, "Behavioral Assessment of Various Control Laws Formulations for Position Tracking of Multi-sectioning Modeled Continuum Robots," 2019 IEEE 7th International Conference on Control, Mechatronics and Automation, ICCMA 2019, 2019, pp. 191–196.